SHIPS AND OFFSHORE STRUCTURES
https://doi.org/10.1080/17445302.2021.1932023

Taylor & Francis
Taylor & Francis Group

A comparative method for scaling SOLAS collision damage distributions based on ship crashworthiness – application to probabilistic damage stability analysis of a passenger ship

Fabien Conti[a], Hervé Le Sourne [b], Dracos Vassalos [c], Pentti Kujala [d], Daniel Lindroth[e], Sang Jin Kim [d] and Spyros Hirdaris [d]

[a]Bureau Veritas, Marine and Offshore, Paris, France; [b]ICAM, Institut Catholique d'Arts et Métiers, Nantes, France; [c]Maritime Safety Research Center, University of Strathclyde, Glasgow, UK; [d]Marine Technology Group, Aalto University, Espoo, Finland; [e]NAPA, Helsinki, Finland

ABSTRACT

SOLAS2020 damage stability regulations are based on probabilistic damage distributions. Those originate from the pooled analysis of collision accidents across a fleet with bias towards cargo ships. This paper introduces a method that accounts for collision-based crashworthiness on ship damage distributions. The method reshapes statistical SOLAS damage distributions for a given ship or structural details for a reference ship section and her reinforced version. Damage reductions may differ depending on ship characteristics and operational scenarios. To mitigate this, a high number of collision scenarios was simulated using the super-element method. It is shown that risk control in terms of damage reduction over the whole range of damages is possible by adding a double hull or by deck reinforcement. Damage reduction is quantified by damage stability analysis of a cruise vessel. It is concluded that installing a double hull on ship vulnerable zones leads to increased A-index.

ARTICLE HISTORY
Received 16 March 2021
Accepted 13 May 2021

KEYWORDS
Passenger ships; crashworthiness; collisions; damage stability; super-element method

NOMENCLATURE

Roman letters

A	Attained Index
B	Ship width
D	Ship depth
$f()$	The survivability function, computed by damage stability software
$g()$	Damage reduction function
$G()$	Non-dimensional damage reduction function
ind_{side}	Damage side, Port side (+1) or starboard side (−1) [-]
L_{ship}	Ship length
L_x	Longitudinal extent of the damage/damage length [m]
L_y	Transversal extent of the damage/penetration [m]
m	Number of crash simulations
n	Number of Monte Carlo damage samples
P_k, P'_k	The probability of occurrence of each individual damage k
S_k, S'_k	The survivability factor for damage k
T	Ship draft
u_0	Striking ship initial surge velocity
X_0	Impact longitudinal position
X_c	Longitudinal position of the centre of the damage [m]
z_{UL}	Damage vertical position upper limit [m]
z_{LL}	Damage vertical position lower limit [m]

Greek letters

α	Collision angle
∇	Ship displacement

Acronyms

CoG	Centre of gravity
DoF	Degree of freedom
FLARE	FLooding Accident REsponse
GM	Metacentric height
LPP	Length between perpendicular
RCO	Risk control option

1. Introduction

In SOLAS2020 (IMO 2017), ship damage stability assessment for collision accidents is based on a probabilistic approach, using distributions from accident statistics. The probabilistic method assumes that each compartment (or group of compartments in a given location in the ship, as 3-dimensional spaces) is associated with a probability of flooding, known as the 'p-factor'.

The derivation of p-factors originates from the HARDER project (1999–2003, Harmonisation of Rules and Design Rationale) during which collision damage statistics were processed to obtain probabilistic damage distributions, in terms of damage longitudinal position, longitudinal extent, transversal extent or upper limit of vertical extent. The mathematical integration of these distributions over box-shaped domains allows expressing the 'p-factors' (as well as 'v-factors') in the known analytical format of SOLAS depending on the ship subdivision.

The SOLAS underlying damage distributions have been obtained by pooling collision accidents of all types of ships available. However, the damage distributions do not explicitly take into account the structural design, or crashworthiness of the ship. Practically, this implies that even if a ship is designed with a high crashworthiness level, no gain is to be expected in terms of safety in the framework of the current regulations. A second consequence is that SOLAS damage distributions embody an 'average' crashworthiness level of the historically damaged ships, which is not necessarily representative of a specific type of ship, or applicable to any type of ship. It is acknowledged that the collision statistics include a high proportion of accidents involving cargo ships and

CONTACT Spyros Hirdaris spyros.hirdaris@aalto.fi; Fabien Conti fabien.conti@bureauveritas.com

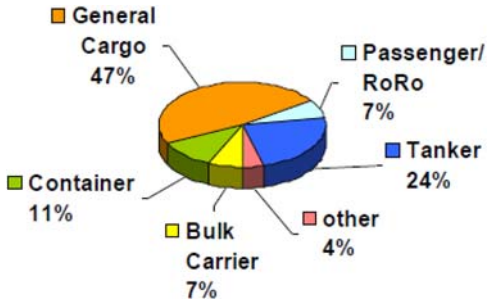

Figure 1. Ship-type breakdown in collision statistics, Papanikolaou et al. (2015) (This figure is available in colour online).

tankers but a limited number of collision accidents involving passenger ships (see Figure 1).

In parallel, considerable research work has been undertaken by various authors in order to derive analytical and numerical methodologies for the estimation of ship structural crashworthiness (Minorsky 1959; Woisin 1979; Pedersen and Zhang 2000; Paik 2007a, 2007b), optimise side shell designs for crashworthiness (Ehlers 2010; Aga 2013) and develop innovative crashworthy solutions with higher energy absorption than conventional designs, involving e.g. corrugated or composite sandwich panels (Kitamura 1997; Lee and Kim 2001; Naar et al. 2001; Törnqvist 2003; Van de Graaf et al. 2004; Ehlers et al. 2007).

The objective of this paper is to present a method that can explicitly take into account the influence of ship structural design and arrangements on damage distributions to be used within the context of probabilistic damage stability assessment, as limited literature is available on this specific topic, see e.g. Lützen (2001) or Egge et al. (2007). For the development of this methodology, which requires the simulation of a large number of collision scenarios, the super-element method is used. For the case studies, conventional structural reinforcements are studied (e.g. increase of plating thickness or material grade), with a specific focus on the consideration of the variability of the damage reduction with respect to the collision scenarios.

2. Methodology

2.1. Overview

SOLAS underlying damage distributions do not explicitly take into consideration ship structural design. Practically, this means that if one considers an arbitrary reference ship and the very same ship with structural reinforcement, both ships will be designed considering the same damage distributions for damage stability, thus leading to the same attained (A) indices (neglecting the additional mass of reinforcement). Nevertheless, one could expect that the safety level in damage stability is different for these two ships, as the extent of damages should be reduced from the reference ship. The objective of the present method is to quantify for a given ship design the modification of SOLAS damage distributions associated with a given reinforcement strategy. Ultimately, this method can be used to assess the efficiency of risk control options (RCOs) or to accept an alternative design. Figure 2 is the flowchart of the method.

This method requires analyses of a very large number of collision scenarios. The simulations cannot be carried out by the finite-element method due to the prohibitive cumulated computation time (Kim et al. 2021a). Instead, simulations have been carried out using the super-element method that is based on modelling the ship by very large-sized structural units (the so-called super-elements), for which closed-form analytical formulations have been derived, see e.g. Amdahl (1982), Wierzbicki and Abramowicz (1983) or Simonsen and Ocakli (1999). These formulations based on experimental data characterise the resistance/energy dissipation of the super-element depending on its type and deformation mechanism.

The actual implementation of the super-element method has been done in an existing programme called SHARP (Le Sourne et al. 2012). Within SHARP, the resistance of each super-element has been derived for ship oblique collisions as explained in Buldgen et al. (2012) and Buldgen et al. (2013). Then, by combining the individual resistances, it is possible to obtain a global evaluation of the ability of both striking and struck ships to withstand a collision event. The SHARP internal mechanics solver has been coupled with an external dynamics programme, namely MCOL. The latter simulates global ship motions, taking into account radiation- and diffraction-induced hydrodynamic actions. Initially, the first version of MCOL was developed and included in LS-DYNA by Mitsubishi LSTC (2018). A few years later, it was entirely rewritten by M. Ferry and H. Le Sourne to take into account large rotational movements driven by the crushing force and hydrodynamic actions (water added mass, wave radiation damping and restoring forces). The solver also accounts for drag damping effects, Ferry et al. (2002). Implemented in LS-DYNA in 2001, this new version was used to simulate the large rotational movement of submarines impacted by surface ships, Le Sourne et al. (2001), and to study surface ships collisions, Le Sourne et al. (2004). A few years later, MCOL programme was also coupled with SHARP solver, Le Sourne (2007) and Le Sourne et al. (2012). Some practical applications of the resulting tool can be found in Paboeuf (2015, 2016).

The coupling between internal mechanics and external dynamics is achieved as follows. At each time step, the structural solver SHARP calculates the three components of the contact force between the striking and the struck ships as well as the three corresponding moments with respect to the ship centre of gravity. The resulting load vector F_C is then transferred to MCOL which solves for each ship the following 6 DoF equation:

$$[M + M_\infty]\,\ddot{x} + G\dot{x} = F_H(x) + F_W(x) + F_V(x) + F_C \qquad (1)$$

where M is the structural mass matrix, M_∞ is the water added mass matrix, x is the earth-fixed position of the ship centre of mass, G is the gyroscopic matrix, F_H is the hydrostatic restoring force vector, F_W is the wave damping force vector and F_V is the viscous force vector. The details for the calculation of G, F_H , F_W and F_V can be found in Le Sourne et al. (2001). The new position, velocity and acceleration at the CoG of the ships, solutions of Eq. (1), are then transmitted back to the structural solver for the next integration time step. It is worth noting that the use of MCOL functionality requires the availability of hydrodynamic data, as shown by Equation (1). This considers the ship added mass, wave damping and hydrostatic restoring matrices, which can be obtained using seakeeping codes like Hydrostar, BV (2019).

To consolidate the reliability of the approach, a benchmark study has been recently carried out in which SHARP/MCOL calculations have been compared to finite element results, Kim et al. (2021b). The main results are summarised in Appendix.

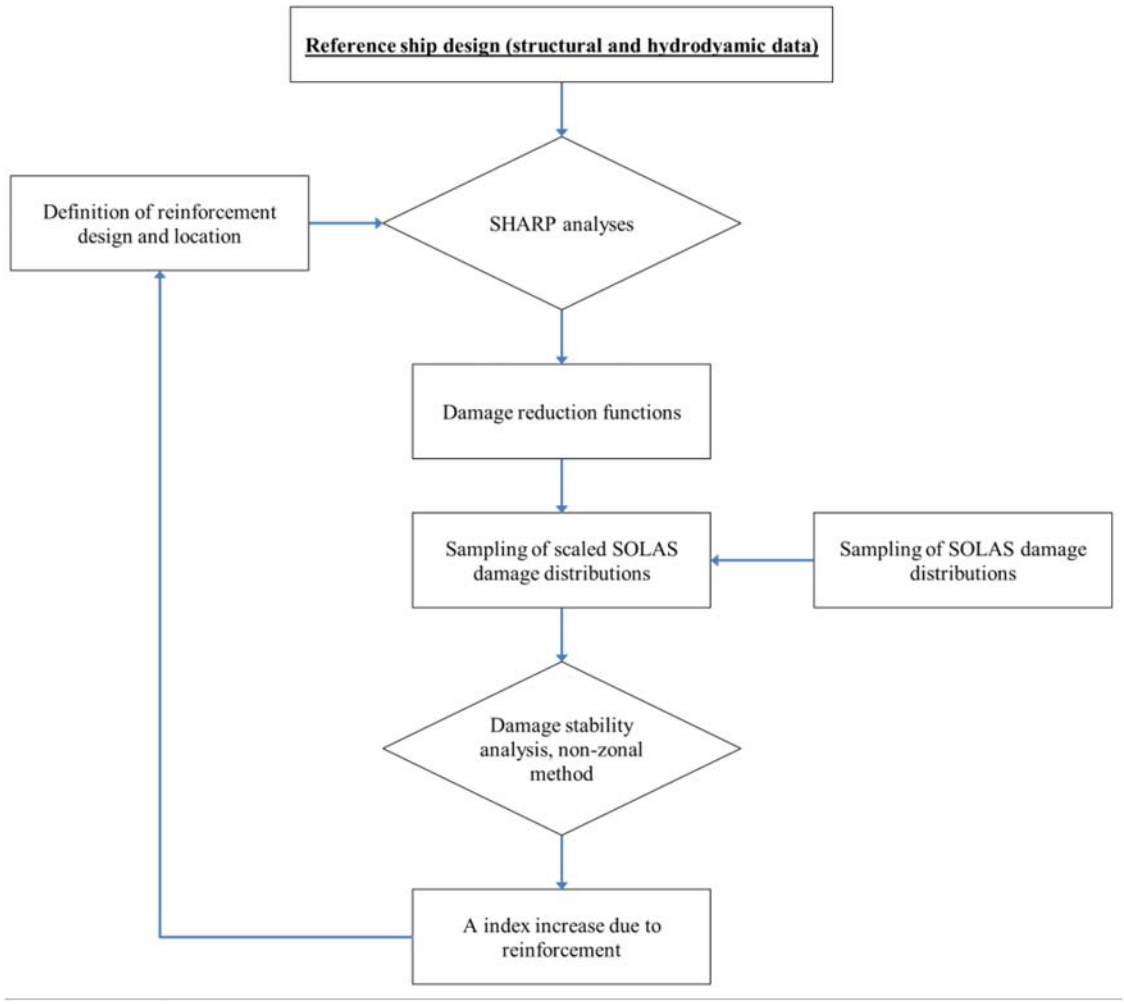

Figure 2. Methodological flowchart (This figure is available in colour online).

2.2. SOLAS geometrical and probabilistic damage description

Geometrically, a collision-type damage is idealised in SOLAS as a box with two faces parallel to the waterplane, two faces parallel to the ship transversal plane and two faces following the hull longitudinal shape at the waterline. Furthermore, the damage box crosses the waterline as well as one side of the ship. In the general case, the damage is modelled using the 6 geometrical parameters (ind_{side}, X_c, L_x, L_y, z_{UL}, z_{LL}), illustrated in Figure 3.

From a probabilistic point of view, SOLAS underlying damage distributions associated with each damage parameter are exemplified in Figures 4–9. It is to be noted that:

- Except for the damage length and penetration, all the random variables describing the damage are assumed to be statistically independent. This entails that all the independent variables can be described by their marginal distributions.
- In the SOLAS framework, the damage lower vertical limit z_{LL} is not considered as a random variable. Instead, a worst-case approach is used for the computation of the s-factor in the case of horizontal subdivision below the waterline. As an extension of the SOLAS framework, Bulian et al. (2019a) introduced a probabilistic description of this variable. This paper considers this extended framework with a probabilistic description of the damage parameter z_{LL}.
- The distributions of the various damage parameters are plotted in their dimensional form, considering the following ship particulars:

$$L_{ship} = 234m/B = 32.2m/T = 7.2m$$

2.3. Principle of the methodology

Let us consider a reference ship for which damage stability analysis shall be carried out considering the above-mentioned damage statistical descriptions. For a structurally reinforced version of this same ship, the damage statistical description would remain the same as the one of the reference ship (since the damage distributions are only driven by ship length, width and draft). The present methodology aims to estimate the damage reduction that would need to be considered for the reinforced ship, from the reference damage by extensive crash analysis. As this methodology is based on a case-by-case comparative analysis of all the potential damages on both ships, it interfaces well with damage stability analyses carried out using the non-zonal Monte Carlo method. Furthermore, this method is very flexible and can address naturally the case of local reinforcements. The use of this non-zonal framework has been, for instance, described by Bulian et al. (2016), Bulian et al. (2019b), Krüger and Dankowski (2019) or Bulian et al. (2020).

For a given ship draft, the calculation of the damage stability attained index using the non-zonal Monte Carlo method relies on:

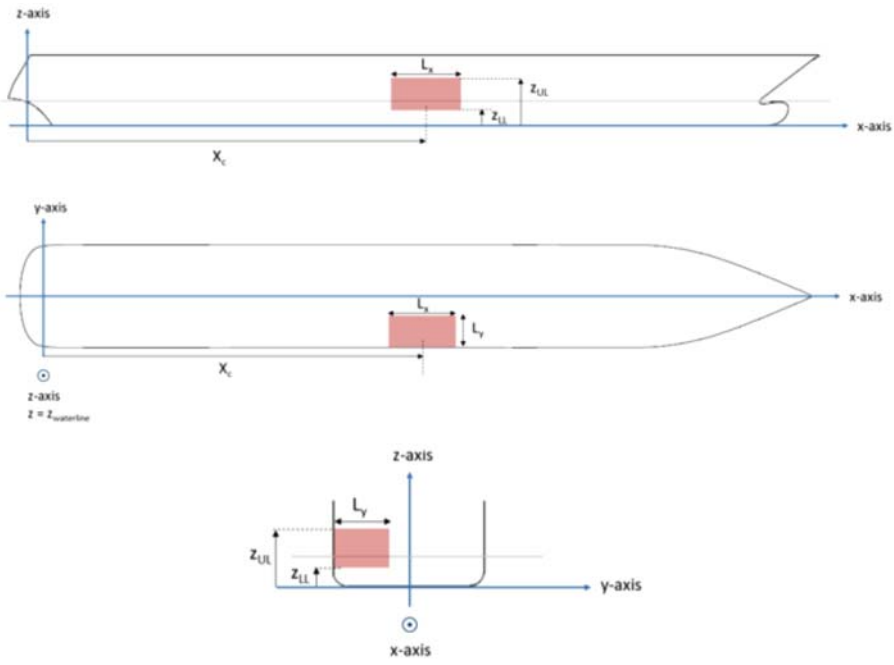

Figure 3. Damage geometrical parameter overview (This figure is available in colour online).

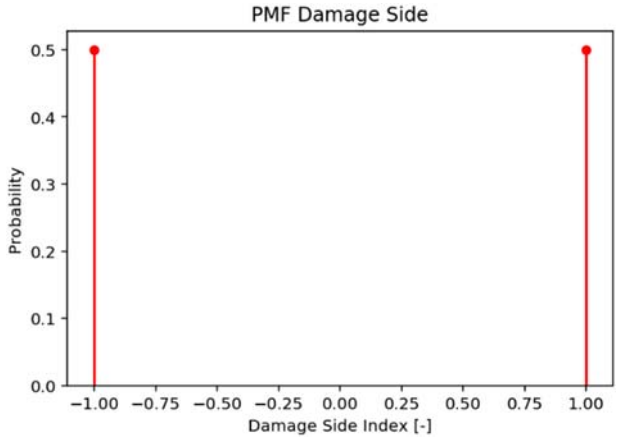

Figure 4. Damage side index probability mass function (This figure is available in colour online).

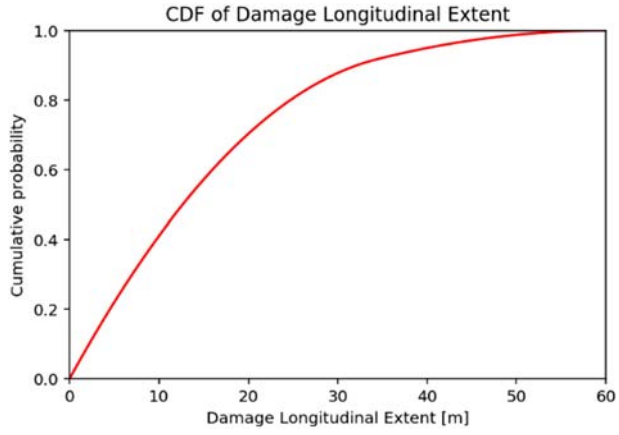

Figure 6. Damage longitudinal extent cumulative distribution function (This figure is available in colour online).

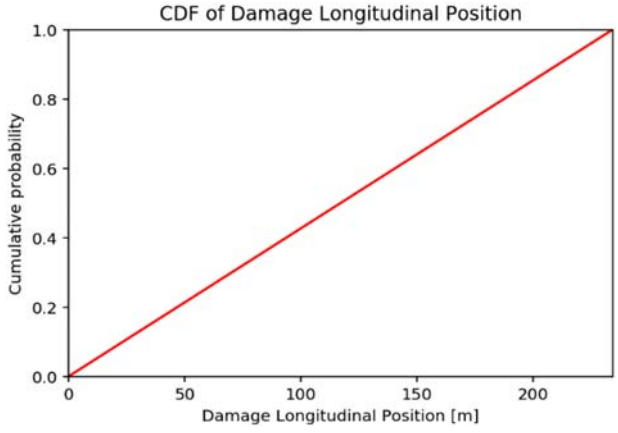

Figure 5. Damage centre longitudinal position cumulative distribution function (This figure is available in colour online).

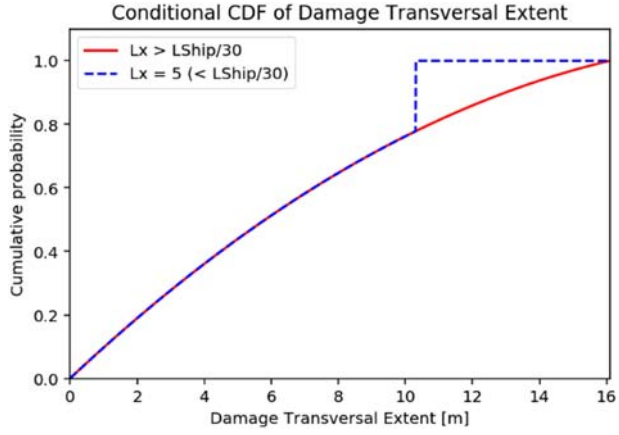

Figure 7. Damage transversal extent conditional cumulative distribution function (This figure is available in colour online).

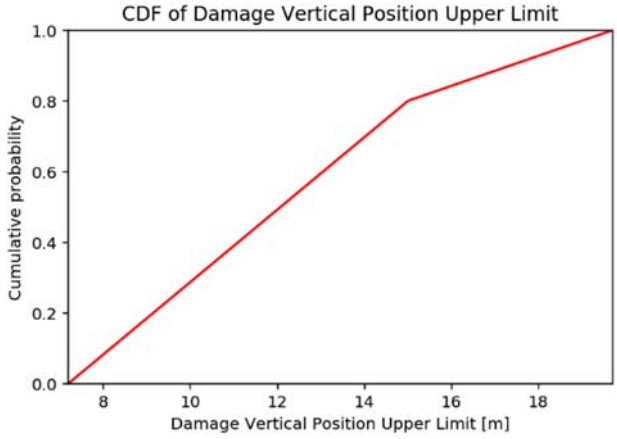

Figure 8. Damage vertical position upper limit cumulative distribution function (This figure is available in colour online).

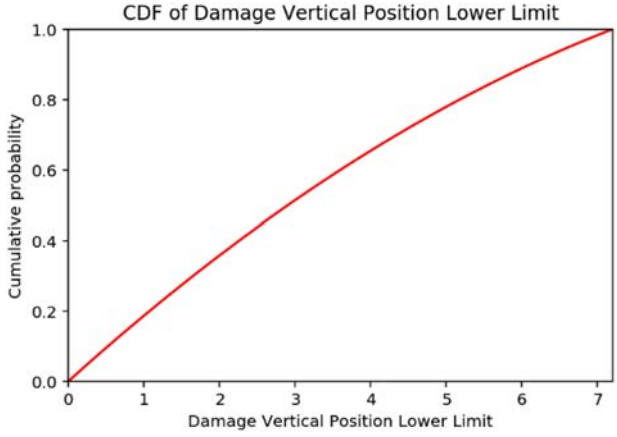

Figure 9. Damage vertical position lower limit cumulative distribution function (This figure is available in colour online).

- The generation of a list of n individual damages $(ind_{side}, X_c, L_x, L_y, z_{UL}, z_{LL})_{k,\ 1\le k\le n}$ sampled according to the above-mentioned distributions, using for instance inverse transform sampling from the cumulative distribution functions.
- The calculation using dedicated software of the survivability factor S_k associated with each individual sampled damage.

Mathematically, the calculation of the partial attained index A for a given draft on the reference ship can be written as follows:

$$A = \sum_{k=1}^{n} P_k.S_k \tag{2}$$

$$S_k = f((ind_{side}, X_c, L_x, L_y, z_{UL}, z_{LL})_k) \tag{3}$$

where $P_k = 1/n$ is the probability of occurrence of each individual damage, S_k is the survivability factor associated with an individual damage and $f()$ is the survivability function, computed by damage stability software.

Similarly, the partial attained index on the reinforced ship can be written as follows:

$$A' = \sum_{k=1}^{n} P'_k.S'_k \tag{4}$$

$$S'_k = f((ind'_{side}, X'_c, L'_x, L'_y, z'_{UL}, z'_{LL})_k) \tag{5}$$

$$(ind'_{side}, X'_c, L'_x, L'_y, z'_{UL}, z'_{LL})_k = g((ind_{side}, X_c, L_x, L_y, z_{UL}, z_{LL})_k) \tag{6}$$

where $P'_k = 1/n$ is the probability of occurrence of each individual damage, S'_k is the survivability factor associated with an individual damage, $g()$ is the damage reduction function and $'$ is the sign that indicates a variable on the reinforced ship.

The objective of the developed methodology is to provide an estimate of the damage reduction function $g()$ based on crash analyses. In order to do so, the considered method consists of the following steps:

- First, a very large number of collision scenarios is run on both the reference and the reinforced ships defined as struck ships. Striking ship types, their drafts, initial velocities, or collision longitudinal position and angle are varied to generate a large matrix of collision scenarios. Following these crash analyses, a collection of n_{simul} damages on both the reference and the reinforced ship was defined:

$$\begin{cases} (ind_{side}, X_c, L_x, L_y, z_{UL}, z_{LL})_{1\le j\le n_{simul}} \\ (ind'_{side}, X'_c, L'_x, L'_y, z'_{UL}, z'_{LL})_{1\le j\le n_{simul}} \end{cases} \tag{7}$$

- Then, the damage reduction function $g(x)$ is estimated. This consists of finding an interpolation model $\tilde{g}(x)$ based on the obtained damages from crash analyses. The task is not trivial since in the more general case, $g(x)$ is a vector-valued function of six variables. Therefore, assessing function $g(x)$ involves assessing six functions of six variables:

$$\begin{cases} (ind_{side}, X_c, L_x, L_y, z_{UL}, z_{LL})_{1\le j\le n_{simul}} \\ (ind'_{side}, X'_c, L'_x, L'_y, z'_{UL}, z'_{LL})_{1\le j\le n_{simul}} \end{cases} \tag{8}$$

The estimation of function $g(x)$ is carried out on a case-by-case analysis depending on the results obtained for the reinforcement studied.

3. Damage simulation

3.1. Reference ship design

The first step of the methodology is to run a very large number of collision scenarios on the reference ship as a struck ship. The aim is to simulate a large range of representative damages. In crash analysis using Super-Element software SHARP, a collision scenario is defined by the following parameters: (a) striking ship type, (b) striking ship initial surge velocity, (c) struck ship initial surge velocity, (d) impact longitudinal position, (e) collision angle, (f) striking ship draft and (g) struck ship draft. For each of these parameters, a range of values has been defined in order to build a load case matrix capable of inducing a large range of damages. 1980 collisions scenarios have been defined by considering the combination of parameters presented in Table 1.

Table 1. Calculation matrix.

Collision parameter	Symbol	Unit	Values
Striking ship type	–	–	11 ships
Striking ship initial surge velocity	u_0	[m/s]	{2, 4, 6, 8, 10}
Impact longitudinal position	X_0	[m]	{95.2, 103.6, 112}
Collision angle	α	[deg]	{30, 60, 45, 90}
Striking ship draft	T^{str}	[m]	$\{T^{str}_{min}, T^{str}_{inter}, T^{str}_{max}, \}$

Table 2. Striking ships general characteristics.

Id	Type	Length overall [m]	Breadth moulded [m]	Max. draft [m]	Depth [m]	Disp. [ton]
1	Cargo Vessel 1	92.2	14	4.9	10	3500
2	OSV	80	17.6	6.85	13.8	3500
3	Chemical Carrier	110	19.5	7.6	10.6	11,064
4	Gas Carrier	155	22.7	6.92	17.95	16,006
5	Cargo Vessel 2	145	15.87	8	11.15	15,415
6	RoRo Vessel	180	30.5	6.8	15.8	22,062
7	Passenger Vessel	251	28.8	6.6	19.35	29,558
8	RoPax Vessel	221	30	6.9	15.32	30,114
9	Bulk Carrier	180	30	10	15	50,000
10	Container Vessel	300	48.2	12.5	24.6	1,19,130
11	Tanker	274	42	14.9	21	1,40,000

With respect to the definition of the collision scenarios, it is to be noted that:

- Since SHARP considers the structural description of one half of the ship (collisions are modelled at port side), the structure of the ship has been considered symmetrical and hence a unique model was used.
- In all simulations, the struck ship is supposed to be at rest (no initial surge velocity). This is in accordance with Lützen (2001) who observed from the collision accident statistics that the most likely surge velocity of the struck ship would be zero. Furthermore, the ship considered for the case study having very limited draft variability, the struck ship was assumed to be at design draft.
- According to the probabilistic damage analysis model, the longitudinal position is independent of all other damage variables. On this basis, only impacts at the mid-ship section were modelled. However, the actual longitudinal position varied so that transverse bulkheads can also be directly hit. In terms of the subsequent damage reduction function estimation, it implies that this function will be as a first approximation, assumed to be independent of the longitudinal position. This assumption is useful to assess the influence of multiple reinforcement strategies, considering various longitudinal positions on the ship. As observed on the loop in Figure 2, once the final reinforcement strategy and longitudinal location are defined, the crash analyses can be rerun taking into account the actual longitudinal location of the reinforcement.
- In simulating collision scenarios, a large range of striking ships is considered, as it drives the damage size obtained but also the relationship between the damage longitudinal, transversal and vertical extents. For the analyses, 11 striking ships of various types and dimensions were modelled. The general characteristics of the striking ships considered represent the world fleet and are shown in Table 2. Model views are shown in Figure 10.

For the case study presented, all the calculations have been carried out considering as reference ship FLOODSTAND SHIP B cruise ship (Luhmann 2009) with the main particulars given in Table 3. The super-element structural description has been modelled for a section that is 100 m long along the ship parallel body and centred on the mid-ship section. All materials have been modelled as rigid-perfectly plastic with S235 mild steel properties (see Table 4). The failure strain – which in SHARP is compared to the averaged tension stress within the super-elements – has been considered equal to 10%. Similar values have been observed by other authors to provide a good fit between super-element predictions and experimental results, Zhang (1999), Lützen (2001), Buldgen et al. (2012). The SHARP super-element model of the struck ship is illustrated in Figure 11. Its hydrodynamic properties as required by MCOL have been obtained using BV Hydrostar software (2019).

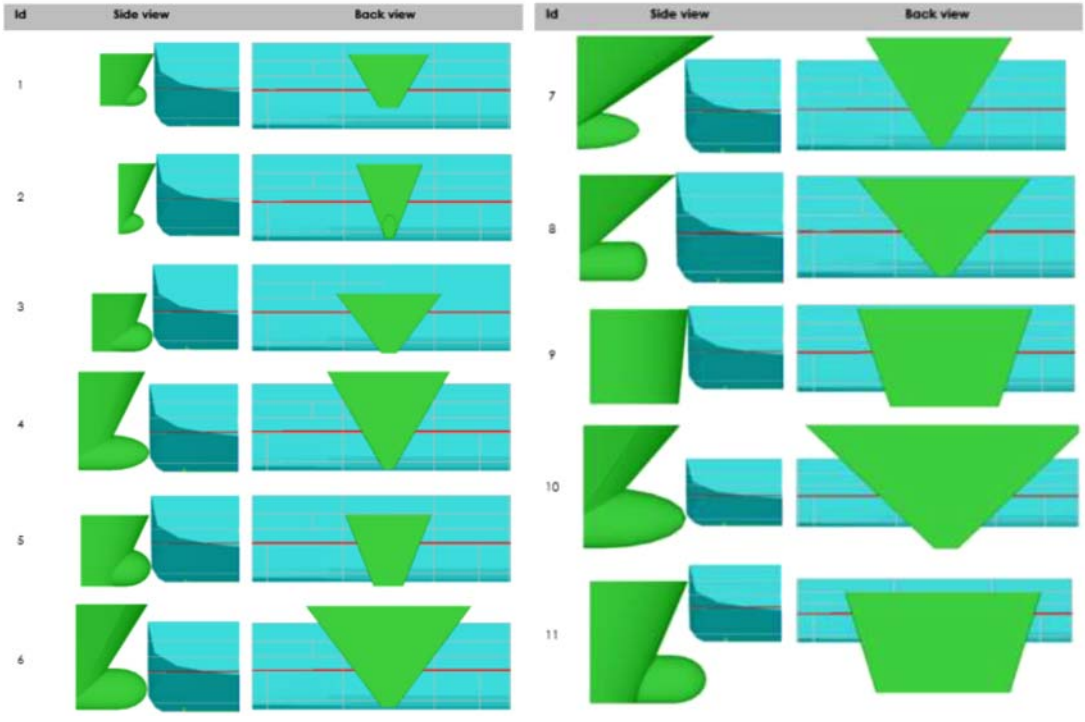

Figure 10. Striking ships views (This figure is available in colour online).

Table 3. Reference ship main particulars.

Parameter	Value
LPP [m]	216.8
Breath moulded B [m]	32.2
Depth D [m]	16
Draft T [m]	7.2
Displacement [tons]	33,923

Table 4. Material parameters considered.

Parameter	Value
Yield strength [MPa]	235
Tensile strength [MPa]	400
Flow stress [MPa]	317.5
Failure strain [-]	10%

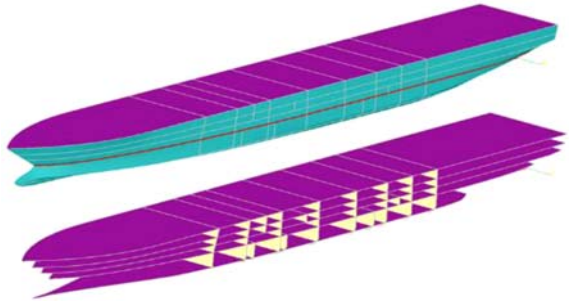

Figure 11. Struck ship SHARP model (This figure is available in colour online).

As far as the striking ship's modelling is concerned, the bow shape has been modelled in SHARP and the ships have been assumed to be rigid. This assumption is conservative regarding the obtained damage reductions (i.e. damage reduction would be higher if the striking ship bow was considered deformable). Also, for the studied ship, this assumption is supported by the FEA computations carried out during the benchmark of SHARP using striking ship 8, which showed a good agreement between the FEA and SHARP results (see Appendix A).

After simulation of all collision scenarios and filtering damages not compatible with SOLAS description (i.e. mainly damages with lower vertical limit above the waterline), it was observed to which extent potential SOLAS damages can be practically simulated. This is demonstrated in Figures 12–15, where the main damage parameters (L_x, L_y, z_{UL}, z_{LL}) are presented by pair plots. Overall, it is

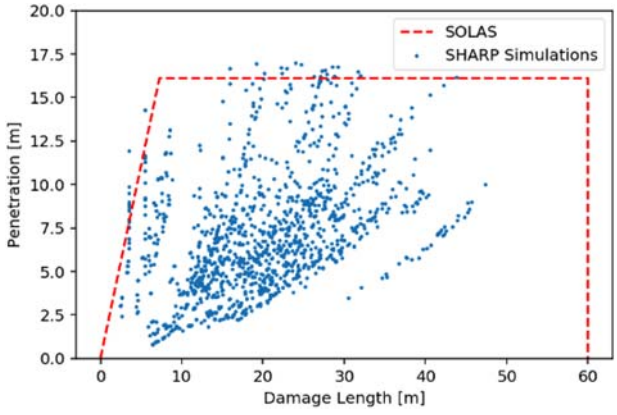

Figure 12. Penetration versus damage length for simulated damages (This figure is available in colour online).

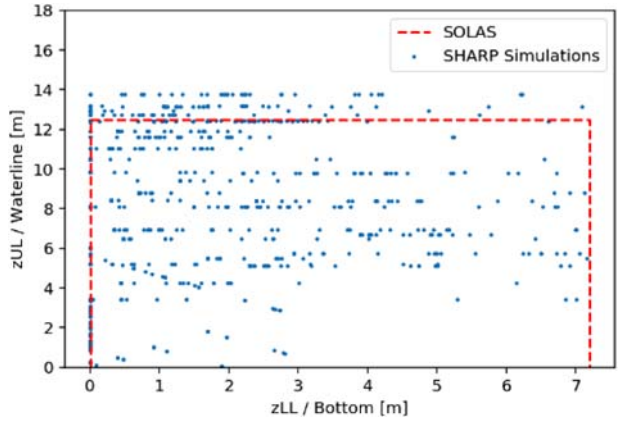

Figure 13. Damage vertical position upper limit versus lower limit for simulated damages (This figure is available in colour online).

deemed that the SOLAS domains are fairly well populated by the simulation results. Some unpopulated areas are discussed below:

- Figure 12 shows that no damages of length higher than 50 m were obtained. A potential explanation is that the calculation matrix could lack some very severe scenarios. Another explanation would be that for the reference ship considered, the SOLAS damage limit of 60 m cannot be physically reached when considering realistic scenarios.
- Figure 12 also shows that longitudinal damages higher than 20 m ($L_x > 20\ m$) with low penetrations ($L_y < 2.5\ m$) cannot be simulated. This may be due to the fact that no initial surge velocity was considered for the struck ship. It could also come from the underlying SOLAS model, which considers that for such type of damages, the longitudinal and transversal extents are independent.
- Figure 13 shows that the domain is well populated due to the large striking ship database. No damages have been simulated with the damage upper limit slightly above the waterline and the damage lower limit slightly below. The simulation of such damages would typically require that the damage is due to the bulb of the striking ship only and that the combination of striking ship draft and bulb height is adequate.
- From Figure 14, it can be noted that no longitudinal damage can be simulated with vertical position just above the waterline. However, this was expected since long damages mainly correspond to the more massive striking ships with high freeboard.
- Figure 15 shows that simulated damages with large penetration have lower vertical limit close to the ship bottom. This was expected given the bow shapes of the striking ships. It is also worth noting that the Bulian et al. (2019a) fully-independent model is considered for the description of the damage vertical position lower limit (i.e. the damage vertical position lower limit is independent of the penetration).

In Figure 16, the results from Figure 12 are shown after clustering the data into either striking ship initial velocity or collision angle. It is observed as expected that the striking ship initial velocity has a significant influence on the damage extent and that the collision angle has a strong impact on the damage length.

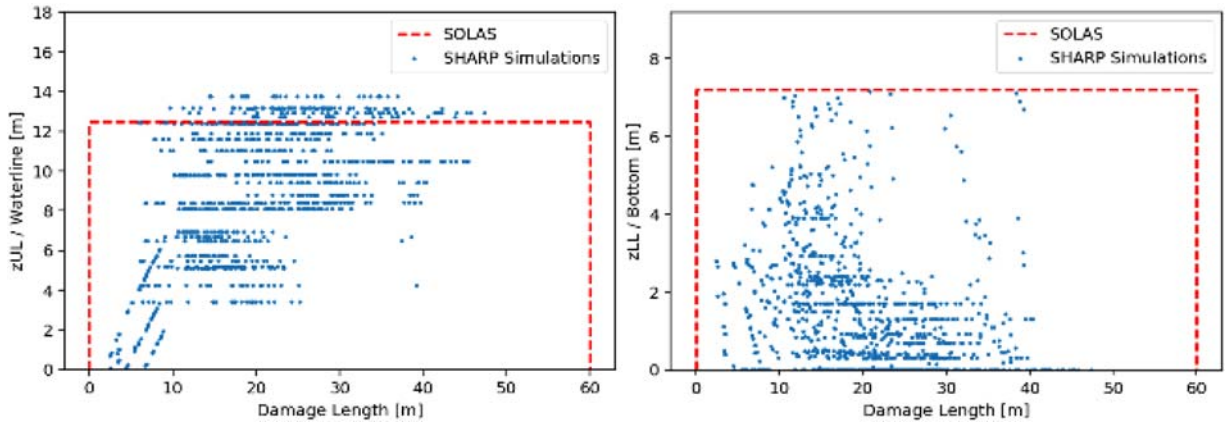

Figure 14. Damage vertical positions versus damage length for simulated damages (This figure is available in colour online).

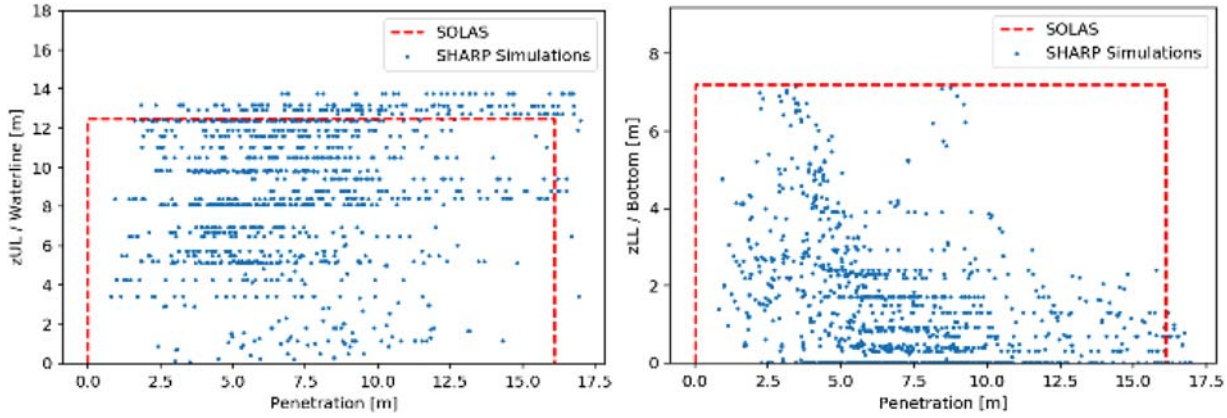

Figure 15. Damage vertical positions versus penetration for simulated damages (This figure is available in colour online).

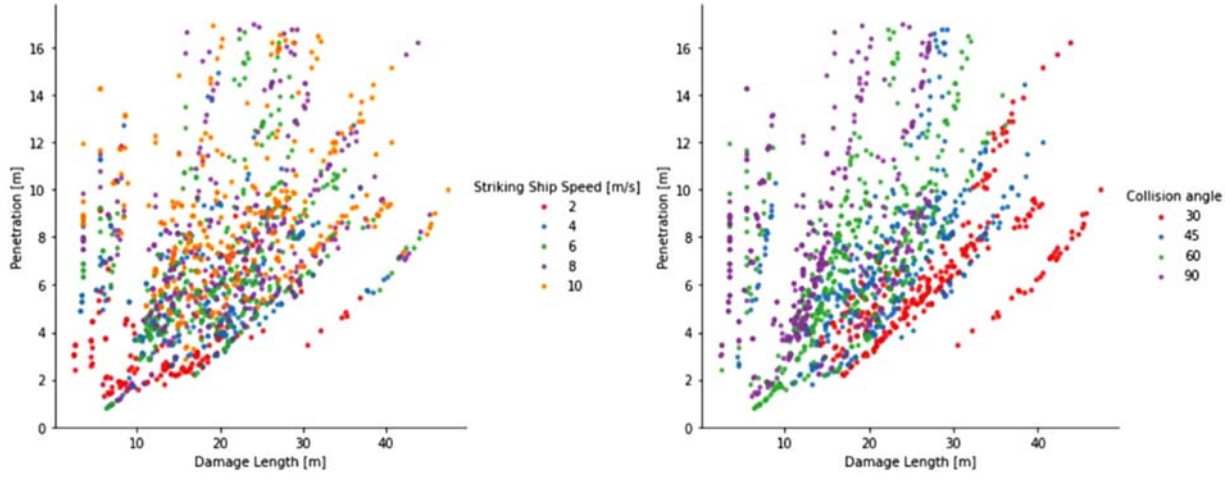

Figure 16. Penetration versus damage length for simulated damages (Left: data clustered by striking ship initial velocity, Right: data clustered by collision angle) (This figure is available in colour online).

3.1. Damage simulation on reinforced ship designs

3.1.1. General

In this section, the assessed reinforcement solutions of the reference ship are presented, with the objective of quantifying the associated damage reduction. Regarding the longitudinal location of the impact, three locations at the mid-ship region have been considered. It was assumed that the damage reduction obtained at amidships can be used for other ship sections with this

reinforcement as per SOLAS philosophy (i.e. the damage size is assumed to be the same whatever the longitudinal position of the damage centre).

Before running the whole calculation matrix, a screening phase has been considered based on a limited number of scenarios (400 scenarios). The purpose of this exercise was to identify the most promising solutions in terms of damage reduction. The following reinforcement solutions have been considered: (a) doubling of hull thickness, namely shell plating and frames, (b) doubling of intermediate decks thickness, namely plating and stiffeners, (c) doubling of transverse bulkheads thickness, namely plating and stiffeners, (d) increase of hull material grade to high strength grade H36, i.e. yield strength of 355 MPa instead of 235 MPa, (e) increase of intermediate decks material grade to high strength grade H36 (i.e. yield strength of 355 MPa instead of 235 MPa); (f) increase of transverse bulkheads material grade to high strength grade H36 (i.e. yield strength of 355 MPa instead of 235 MPa) and (g) addition of a double hull (1 m width with 7 mm thick transverse plates with a spacing of 2.8 m). For each reinforcement solution studied, the reference structural and material models were updated accordingly. Whenever material grade increase was studied, the material yield and tensile stresses were modified while the failure strain and failure criteria of the reference model were kept.

The results obtained show that the increase of the material grade of the hull has a very limited impact. Increasing the material grade of intermediate decks or transverse bulkheads has an even lower impact on the damage reduction. The explanation is that the hull plates in way of the super-element region may be loaded out-of-plane. For such case, the energy dissipation is directly linked to the material flow stress. However, increasing the hull material grade has a limited impact on the damages since the energy dissipated by the hull remains small compared to the total energy dissipated, especially when the penetration is large. Regarding the increase of material grade for decks or transverse bulkheads, these structures are modelled by a super-element corresponding to a plate loaded in-plane on its free-side and for which energy dissipation is due to concertina deformation mode. The finding that increasing the material grade for these structures has negligible impact on the damage reduction is believed to be due to the fact that the failure threshold of these super-elements (due to either excessive strain or excessive forces at weld and which has a critical impact on the energy dissipation) is unaffected by the material flow stress increase. Consequently, reinforcements involving material grade increase have not been further studied. The screening analysis has also shown that the doubling of transverse bulkheads thickness only had a modest impact on the damage reduction, due to the large spacing of these elements (about 12–17 m).

After pre-screening, the following reinforcements have been studied considering the full calculation matrix: doubling of hull thickness (shell plating and frames), doubling of intermediate decks thickness (shell plating and stiffeners) and addition of double hull (1 m width with 7 mm thick transverse plates with a spacing of 2.8 m). For each reinforcement type, the whole calculation matrix was run, with the assumption that the hydrodynamic behaviour is unaffected by the additional weight of the reinforcement (i.e. identical MCOL matrices considered for all the calculations). Before post-processing the results, they have been filtered to exclude non-converged scenarios as well as scenarios yielding unphysical results, e.g. peaking force in a super-element.

Equation (8) has presented the damage reduction functions to be fitted from the calculations in their more general shape. From the observation of calculation results, the damage reduction functions have been rewritten (Equation (9)) in a non-dimensional shape. These new sets of relationships further assume that the damage side, longitudinal position and upper vertical position are not affected by the reinforcement and that the damage reductions (longitudinally, transversally or vertically) can be expressed as functions of the penetration L_y only. This is supported by the observation of the calculation results, which have shown no correlation between the damage reduction ratios and the damage variables except for the penetration.

$$\begin{cases} G_3(L_y) = \dfrac{L'_x}{L_x} \\ G_4(L_y) = \dfrac{L'_y}{L_y} \\ G_6(L_y) = \dfrac{z'_{UL} - z'_{LL}}{z_{UL} - z_{LL}} \end{cases} \tag{9}$$

3.1.2. Increased hull thickness

For the case of reinforced hull by thickness increase (from 15 mm shell plating to 30 mm in average), the obtained results are shown in Figure 17. The results are presented in terms of damage reduction ratios versus penetration on the reference ship design, where blue markers represent each calculated collision scenario. It can be observed that the higher the penetration, the lower the associated reduction ratio. Physically, this may be attributed to modest penetrations for which the portion of the dissipated energy due to the hull can be significant. On the contrary, for large penetrations, the portion of the dissipated energy due to the hull is negligible (the energy is mostly dissipated by decks and transverse bulkheads in this case), which explains that hull reinforcement also has a negligible impact on the damage size reduction. To quantify the relationships linking each damage size reduction ratio to the penetration, data binning has been considered. Accordingly, the penetration was binned into six categories for which the average reduction ratio is computed (red markers in the left part of Figure 17). Using this representation, it appears that the relationships linking each damage size reduction ratio to the penetration can be modelled by a parabolic fit (red line in the right part of Figure 17). The analytical expressions obtained for the damage reduction functions are given in Table 5.

3.1.3. Increased intermediate decks thickness

The results obtained for reinforced intermediate decks by thickness increase (from 6 mm shell plating to 12 mm in average for decks located between inner bottom and main deck) are shown in Figure 18. After data binning by penetration categories (see red markers in Figure 18), no evident correlation between the damage reduction ratios and the penetration on the reference ship was observed. Physically, this can be explained by the fact that the energy dissipated by the decks (which is a significant part of the total dissipated energy) increases with increasing penetration so that the effectiveness of the reinforcement is maintained whatever the penetration. Therefore, in terms of damage reduction functions fitting, a simple scalar model independent of the penetration and based on the average calculation results is proposed (Table 6).

3.1.4. Addition of double hull

The results obtained in the case of the addition of a double hull (1 m width with 7 mm thick transverse plates with a spacing of 2.8 m) are shown in Figure 19. Again, after data binning by penetration categories, no evident correlation between the damage reduction ratios and the penetration on the reference ship was observed. Qualitatively, this could be attributed to the striking

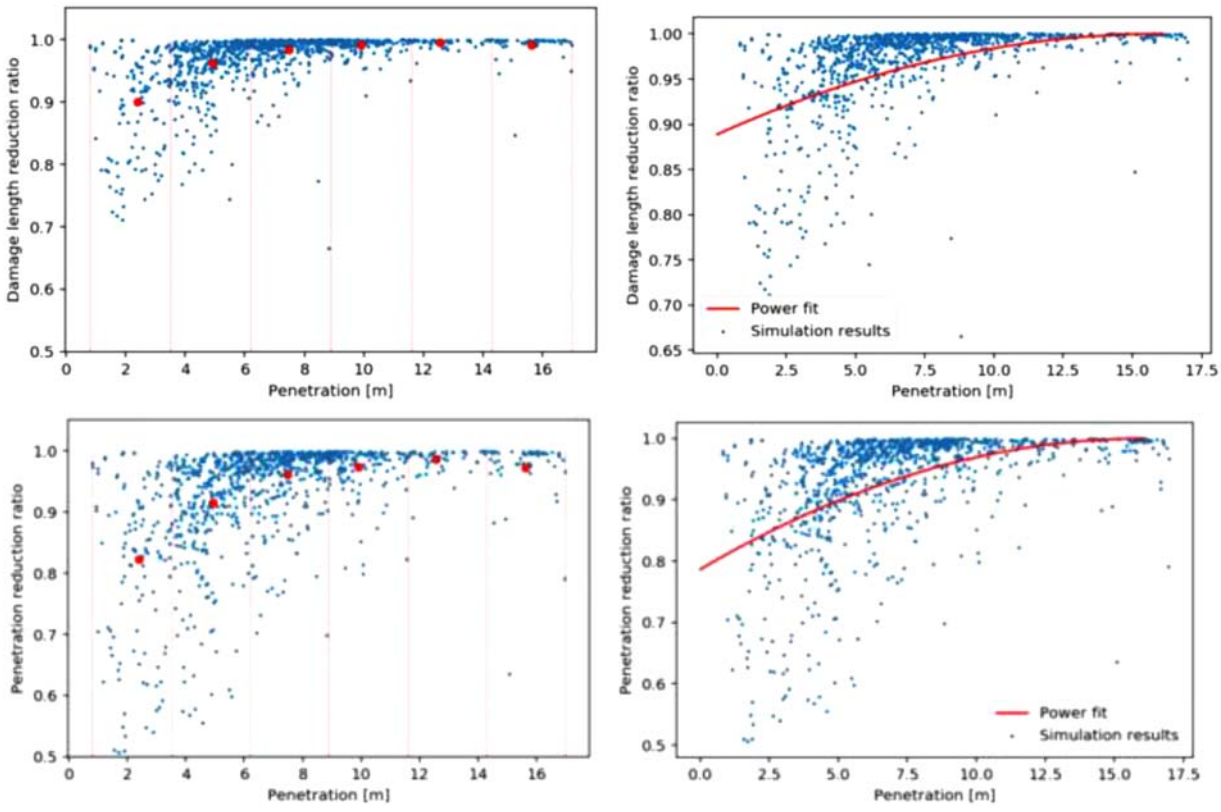

Figure 17. Damage reduction ratios, reinforced hull thickness (Up: damage length, Bottom: penetration) (This figure is available in colour online).

Table 5. Models for damage size reduction ratios, reinforced hull thickness.

	Damage size reduction ratio		
Parameter Model	Damage length	Penetration $G_i(L_y) = C_1.L_y^2 + C_2.L_y + C_3$	Damage height
$G_i(L_y) =$	$\frac{L'_x}{L_x}$	$\frac{L'_y}{L_y}$	$\frac{z'_{UL} - z'_{LL}}{z_{UL} - z_{LL}}$
C_1	-4.29×10^{-4}	-8.24×10^{-4}	-3.27×10^{-4}
C_2	1.38×10^{-2}	2.65×10^{-2}	1.05×10^{-2}
C_3	0.89	0.79	0.92

ship bow shape that activates additional super-elements (transverse webs and intersections in the double hull), as the penetration increases. These super-elements, in turn, contribute to energy dissipation (see example in Figure 20 for 90° collision). The situation is different for the reinforced hull thickness, for which the energy dissipated by the hull stops increasing when the hull is breached. Therefore, for the fitting of the damage reduction function in the case of the double hull, a simple scalar model independent of the penetration and based on the average calculation results is proposed (Table 7).

Table 6. Models for damage size reduction ratios, reinforced intermediate decks thickness.

	Damage size reduction ratio		
Parameter Model	Damage length	Penetration $G_i(L_y) = C_1$	Damage height
$G_i(L_y) =$	$\frac{L'_x}{L_x}$	$\frac{L'_y}{L_y}$	$\frac{z'_{UL} - z'_{LL}}{z_{UL} - z_{LL}}$
C_1	0.93	0.83	0.95

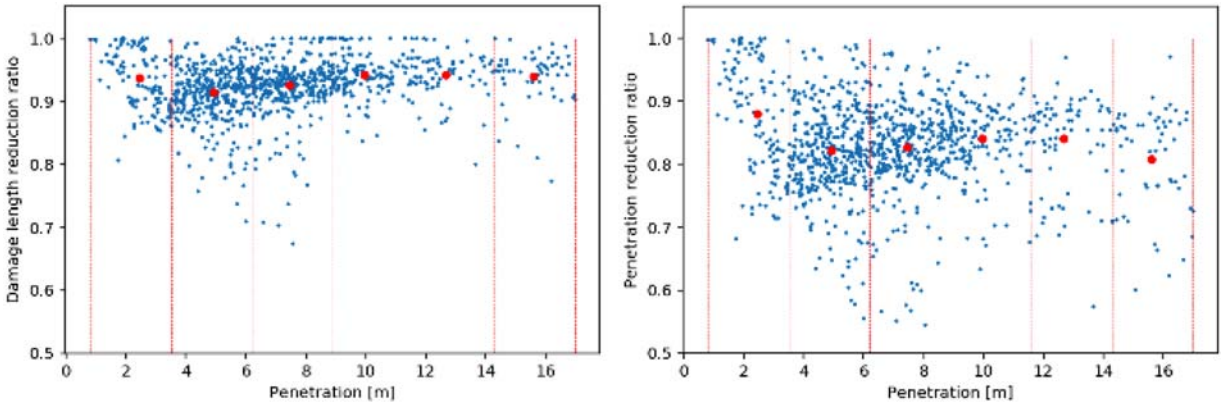

Figure 18. Damage reduction ratios, reinforced intermediate decks thickness (Left: damage length, Right: penetration) (This figure is available in colour online).

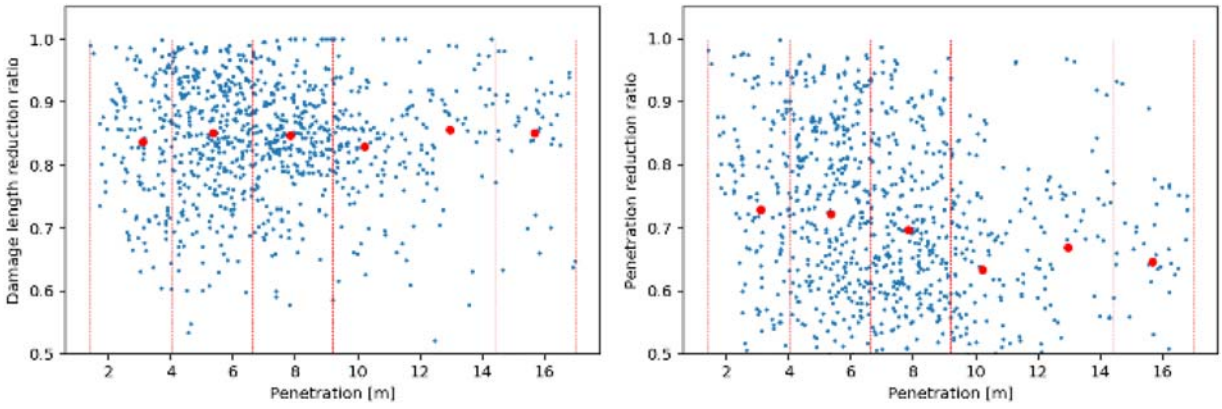

Figure 19. Damage reduction ratios, addition of double hull (Left: damage length, Right: penetration) (This figure is available in colour online).

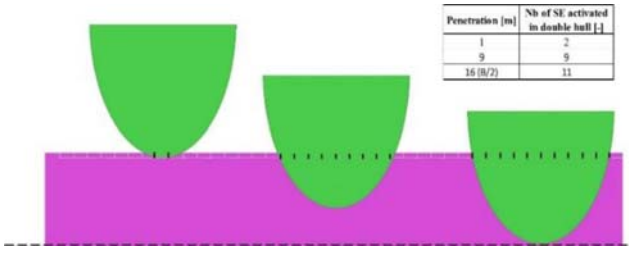

Figure 20. Double hull super-elements activation with penetration increase (This figure is available in colour online).

Table 7. Models for damage size reduction ratios, addition of double hull.

	Damage size reduction ratio		
Parameter Model	Damage length	Penetration $G_i(L_y) = C_1$	Damage height
$G_i(L_y) =$	$\frac{L'_x}{L_x}$	$\frac{L'_y}{L_y}$	$\frac{z'_{UL} - z'_{LL}}{z_{UL} - z_{LL}}$
C_1	0.85	0.70	0.89

3.2. A-index calculation example

As a case study for the implementation of the methodology using the non-zonal Monte Carlo method, damage stability analysis was carried out considering the damage reduction ratios obtained with the 1-m width double-hull design. The reinforcement was applied in way of 3 zones contributing the most to the loss of A-index (see Figure 21). The flooding was calculated statically (not simulated) in a similar manner as SOLAS damage calculations. The calculation was done using NAPA Software. In SOLAS damage calculations, all initially breached rooms are instantaneously broken and open to sea, and the calculation is done in calm water for an empty ship. Consequently, a variation in the size of an individual breach will only affect the outcome of the damage stability calculation when the rooms hit by this breach changes (increases or decreases). In terms of computation time, this static damage stability analysis is fast, as it does not need to calculate all breaches individually (some breaches will result in the same broken rooms, and only one of each individual room combination needs to be calculated).

In the modified model, the alteration of the ship weight, CoG position and GM due to the reinforcement have been neglected, and the calculations have been performed for one draft (thus leading to partial A-index assessment). The added void spaces were limited to above the double bottom. Thus, they were assumed not to affect the existing cross flooding arrangement. Other existing intermediate stages modelled were changed to A-class connections. No additional cross-flooding or down-flooding was added. The methodology applied for damage reduction is described in Section 2.3. At first, a list of $n = 10,000$ reference damages were sampled in accordance with the distributions given in Section 2.2. This list formed the reference damages. Then, a modified damage list was created by scaling all the damages located in the reinforced zones using the damage size reduction ratios obtained by post-processing of the crash analysis results. For the specific case of damages partially located on the reinforced zones, the applied reduction factors were scaled proportionally to the percentage of the damage length, which actually intersects the reinforced zone. The obtained result is shown in Table 8.

4. Discussion

In Figures 18 and 19, a significant scatter of data can be observed. This could be expected given the very high number of collision scenarios with various collision parameters that were considered (in particular various striking ships impact different structural elements). Also, it is to be noted that contrary to non-coupled crash analysis methods (in which the rigid body motions as well as the energy to be dissipated by the structure are pre-computed), the calculations are coupled in SHARP. This entails that the reinforcements alter the resolution of the rigid body motions as well as the energy dissipated. These results underline that a large range of collision scenarios should be considered to ensure that the method is effective. A similar conclusion was reached by Törnqvist (2003), which highlighted that improved energy absorption capabilities shall be evaluated for a particular ship on a particular route.

As the data from Figures 18 and 19 are not dependent on the penetration, they can be visualised by histograms. With the present method, collision scenarios are arbitrary. Thus, such visualisation may not be interpreted in a probabilistic context. However, it may provide useful information regarding the way the data are actually scattered. Figure 22 shows that despite the relatively high scatter of the data observed in terms of extreme values, a peak in the distributions emerges so that a large amount of data remains close to the average values considered in the definition of damage reduction functions (Section 3.2.4). It is also worth noting that

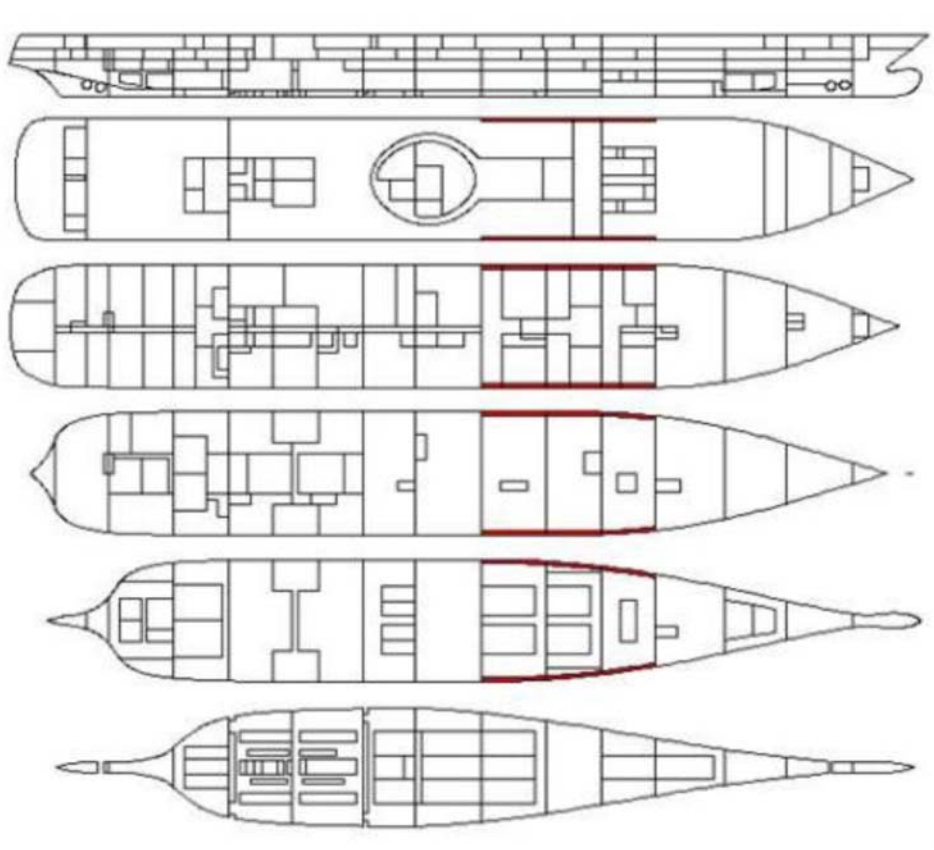

Figure 21. General layout with 3 zones reinforced with double hull (This figure is available in colour online).

Table 8. Results of damage stability analysis.

Model	Partial A-index	Increase wrt. Reference model
Reference model	0.876	–
Reinforced model	0.891	+1.7%

the scatter of the results appears to be higher when a double hull is added. This could be attributed to the calculation method. For the double hull model, the super-element breakdown is different than the reference model (e.g. decks super-element of the reference model is subdivided in the double hull model due to the presence of the double hull), which alters the forces carried by each individual super-element.

The influence of structural reinforcement on the damage stability attained index is seen in Table 8. For the case study presented, despite quite significant damage reduction, the increase of partial A-index remains limited. This could be attributed to the fact that even if the penetration reduction is quite significant (−30%), the damage length reduction is less important (−15%). Thus, the increase of partial A-index is mainly due to the cases where a flooded zone becomes non-flooded due to the damage length reduction. This result demonstrates that in order for a crashworthy solution to be effective at increasing the SOLAS attained index, very significant damage reductions should be targeted for the whole spectrum of SOLAS potential damages. In the present work, the emphasis has been laid on the development of a comparative methodology linking crashworthiness and probabilistic damage stability analyses. For the case studies, the chosen reinforcement strategies (increase of plating thickness, material grade, addition of double-hull) have been driven by the possibilities of the SHARP software version used, where structural super-elements library includes hull panels, decks, transversal bulkheads, longitudinal bulkheads, intersections or stiffeners. As future work, the methodology could be extended in order to assess the increase of attained index resulting from the consideration of more efficient crashworthy solutions such as sandwich structures with corrugated plates or foam between the skins. This work would involve the development of a new super-element type, which constitutive penetration–deformation energy relationship would be specified by the user following finite-element analysis or experimental testing.

5. Conclusions

In SOLAS (2020), ship probabilistic damage stability assessment is based on predefined damage distributions. This implies that ship crashworthiness is not explicitly taken into account.

In this paper, a novel methodology has been developed and tested in order to assess the influence of ship structural design for use in the frame of damage stability analyses. The methodology presented aims to scale SOLAS damage distributions by comparison between a reference ship design for which SOLAS damage distributions are considered and her reinforced version. This is achieved by simulating a high number of collision scenarios on both ships by varying the parameters defining the collision scenarios, such as the type of striking ship, the surge velocity of the striking ship, the collision angle or the draft of the ships into collision. In total, the collision scenario matrix included a number of 1980 collision cases. Due to the prohibitive cumulated computation time required by simulations considering

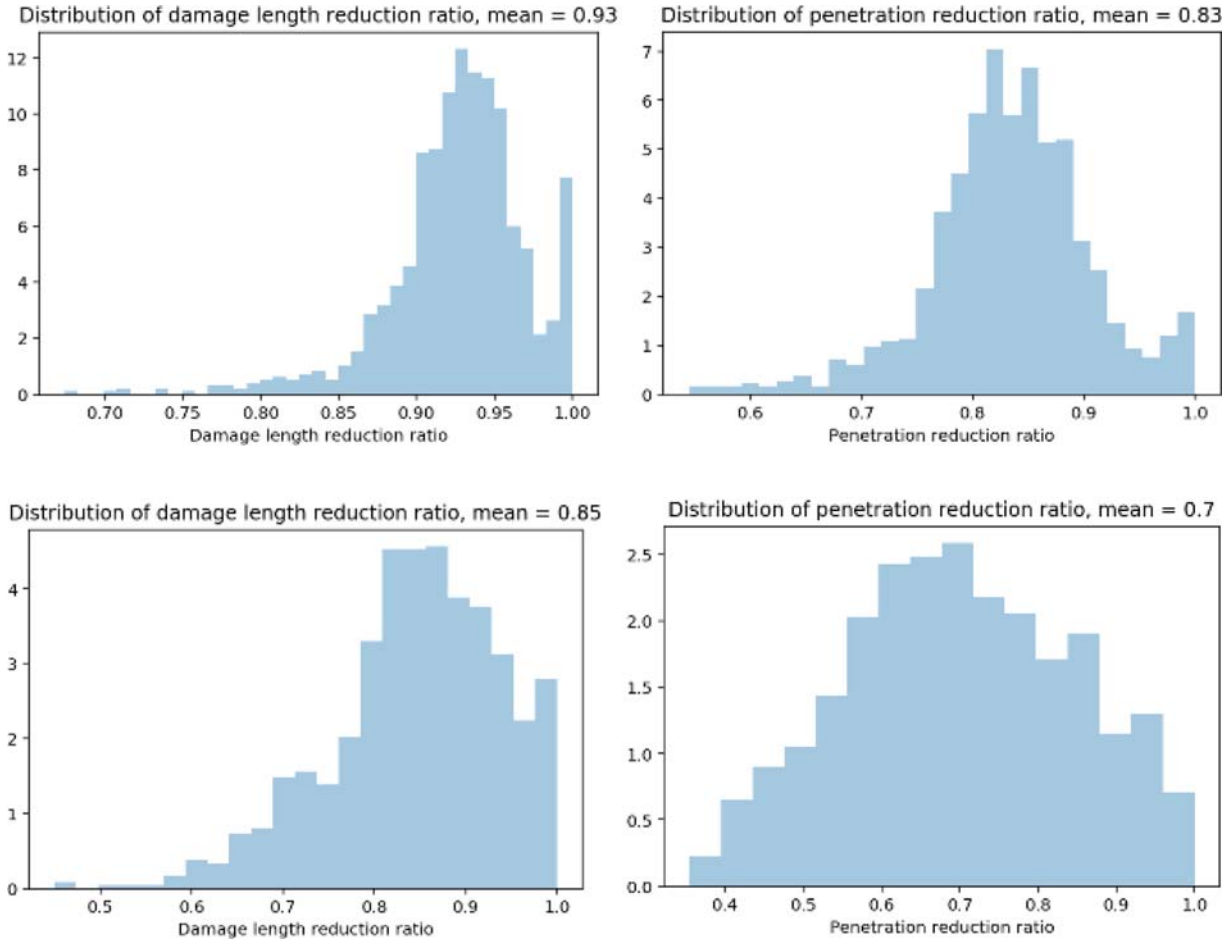

Figure 22. Damage reduction ratio histograms (Up: reinforced hull thickness, Bottom: addition of double hull) (This figure is available in colour online).

the finite-element method, the collision scenarios were simulated using the super-element method (SHARP software), which provides fast and accurate estimations of the resulting damages. For reference, the computation of a single collision scenario typically runs in 1–2 min using SHARP while using the finite-element analysis method can lead to computation times of several days.

The methodology has been tested on a cruise ship, for which multiple reinforcement solutions – including material grade increase and thickness increase – have been studied. In particular, detailed analyses have been carried out for two hull reinforcement strategies: (a) hull reinforcement by increase of the thickness of the side shell plating and stiffeners and (b) hull reinforcement by addition of a double hull with a width of 1 m. Solution (a) has shown to be effective for damage reduction only for limited penetrations. This could be explained by the fact that for large penetrations, the portion of the dissipated energy due to the hull becomes low as a large part of the energy is dissipated by the decks. Solution (b) has shown to be an effective measure for damage reduction, with no significant loss of efficiency with increasing penetration. This could be attributed to the fact that additional super-elements (transverse webs and intersections in the double hull) are activated, as the penetration increases. For all the simulations performed, it has been observed that the damage reduction obtained can differ among the collision scenarios, thus showing that it is important to consider a large range of representative collision scenarios.

For solution (b), a damage stability analysis using the non-zonal Monte Carlo method was carried out, considering the damage reduction ratios obtained from crash analyses for three ship vulnerable zones. It was observed that despite quite significant damage reduction (−30% in penetration and −15% in damage length), the increase of partial A-index remained limited (+1.7%).

Acknowledgements

The authors express their gratitude for this support. The views set out in this paper are those of the authors and do not necessarily reflect the views of their respective organisations or of the FLARE consortium.

Disclosure statement

No potential conflict of interest was reported by the author(s).

Funding

The research presented in this paper has received funding from the European Union project FLooding Accident REsponse (FLARE) number 814753 under H2020 programme.

ORCID

Hervé Le Sourne http://orcid.org/0000-0002-2142-0210
Dracos Vassalos http://orcid.org/0000-0002-0929-6173
Pentti Kujala http://orcid.org/0000-0003-2665-9957
Sang Jin Kim http://orcid.org/0000-0001-9317-0479
Spyros Hirdaris http://orcid.org/0000-0002-4700-6325

References

Aga HL. 2013. Assessment of structural requirements related to LNG fuel tanks. Master Thesis, Department of Marine Technology, Norwegian University of Science and Technology.

Amdahl J. 1982. Energy absorption in ship – platform impact. PhD Thesis, Department of Marine Technology, Norwegian Institute of Technology.

Buldgen L, Le Sourne H, Besnard N, Rigo P. 2012. Extension of the super-element method to the analysis of the oblique collision between two ships. Marine Struct. 29:22–57.

Buldgen L, Le Sourne H, Rigo P. 2013. A simplified analytical method for estimating the crushing resistance of an inclined ship side. Marine Struct. 33:265–296. doi:10.1016/j.marstruc.2013.06.005.

Bulian G, Lindroth D, Ruponen P, Zaraphonitis G. 2016. Probabilistic assessment of damaged ship survivability in case of grounding: development and testing of a direct non-zonal approach. Ocean Eng. 120:331–338.

Bulian G, Cardinale M, Francescutto A, Zaraphonitis G. 2019a. Complementing SOLAS damage ship stability framework with a probabilistic description for the extent of collision damage below the waterline. Ocean Eng. 186:106073. doi:10.1016/j.oceaneng.2019.05.055.

Bulian G, Cardinale M, Dafermos G, Eliopoulou E, Francescutto A, Hamann R, Lindroth D, Luhmann H, Ruponen P, Zaraphonitis G. 2019b. Considering collision, bottom grounding and side grounding /contact in a common non-zonal framework. Proceedings of the 17th International Ship Stability Workshop.

Bulian G, Cardinale M, Dafermos G, Lindroth D, Ruponen P, Zaraphonitis G. 2020. Probabilistic assessment of damaged survivability of passenger ships in case of grounding or contact. Ocean Eng. 218:107396. doi:10.1016/j.oceaneng.2020.107396.

BV (2019). Hydrostar for experts user manual. Paris: Bureau Veritas.

Egge ED, Zhang L, Scharrer M. 2007. Simplified approval procedure by introduction of a normalized energy function (NEF) in line with SOLAS regulations. Proceedings of 4th International Conference on Collision and Grounding of Ships, Hamburg.

Ehlers S, Klanac A, Tabri K. 2007. Increased safety of a tanker and RO-PAX vessel by implementing a novel sandwich structure. Proceedings of 4th International Conference on Collision and Grounding of Ships: ICCGS 2007, Hamburg, Germany, 109−117.

Ehlers S. 2010. A procedure to optimize ship side structures for crashworthiness. Proceedings of the Institution of Mechanical Engineers, Part M: Journal of Engineering for the Maritime Environment. 224.

Ferry M, Le Sourne H, Besnier F. 2002. MCOL theoretical manual. Principia Marine, Nantes.

HARDER. Harmonization of rules and design rationale. EU Contract No. G3RD-CT-1999-00028.

IMO. 2017. Resolution MSC.421 (98), Amendments to the International Convention for the Safety Of Life At Sea, 1974, as amended, 15 June.

Krüger S, Dankowski H. 2019. A Monte Carlo based simulation method for damage stability problems. Proceedings of the ASME 2019 38th International Conference on Ocean, Offshore and Arctic Engineering OMAE2019 June 9–14, 2019, Glasgow, Scotland, UK.

Kitamura O. 1997. Comparative study on collision resistance of side structures. Marine Technol. 34(4):293–308.

Kim SJ, Kõrgersaar M, Ahmadi N, Taimuri G, Kujala P, Hirdaris S. 2021. The influence of fluid structure interaction modelling on the dynamic response of ships subject to collision and grounding. Marine Struct. 75:102875.

Kim SJ, Taimuri G, Kujala P, Conti F, Le Sourne H, Pineau JP, Looten T, Bae H, Mujeeb-Ahmed MP, Vassalos D, et al. 2021b. Comparison of numerical approaches for structural response analysis of passenger ships in collisions and groundings, Marine Structures (Under review).

Le Sourne H, Donner ER, Besnier F, Ferry M. 2001. External dynamics of ship-submarine collision – 2nd International Conference on Collision and Grounding of Ships, 137–144, Copenhagen.

Le Sourne H, Besnier F, Couty N. 2004. LS-DYNA applications in shipbuilding – 4th International LS-DYNA Conference, Paris (lecturer in plenary session).

Le Sourne H. 2007. A ship collision analysis program based on super-element method coupled with large rotational ship movement analysis – 4th International Conference on Collision and Grounding of Ships, 131–138, Hamburg.

Le Sourne H, Besnard N, Cheylan C, Buannic N. 2012. A ship collision analysis program based on upper bound solutions and coupled with a large rotational ship movement analysis tool. J Appl Math. doi:10.1155/2012/375686.

Le Sourne H, Pineau J-P, Kim SJ, Conti F, Kaydihan L, Bae E, Vassalos D, Kujala P, Hirdaris S. 2021. A comparison of crashworthiness methods for the assessment of ship damage extents. 1st International Conference on the Stability and Safety of Ships and Ocean Vehicles.

Lee J, Kim J. 2001. A comparative study of the double hull structures for collision energy absorbation systems. J Ship Ocean Technol. 5(4):19–28.

LSTC. 2018. LS-DYNA keyword user's manual. California: Livermore Software Technology Corporation.

Luhmann H. 2009. Floodstand WP1: concept ship design B.

Lützen M. 2001. Ship collision damages, PhD Thesis, Department of Mechanical Engineering, Technical University of Denmark.

Minorsky VU. 1959. An analysis of ship collisions with reference to protection of nuclear power plants. J Ship Res. 3:1–4.

Naar H, Kujala P, Simonsen B, Ludolphy H. 2001. Comparison of the crashworthiness of various bottom and side structures. Proc. of 2nd International Conference on Collision and Grounding of Ships, Copenhagen, 8(1):179–188.

Paboeuf S, Le Sourne H, Brochard K, Besnard N. 2015. A damage assessment tool in ship collisions. Proceedings of 3rd RINA Damaged Ship Conference, London, March 2015.

Paboeuf S, Uzögüten HO, Le Sourne H, Wa N. 2016. Crashworthiness of an alternative construction within the scope of A.D.N. Regulations using super-elements method. Proceedings of the 7th International Conference on Collision and Grounding of Ships, 247–254, Ulsan.

Paik JK. 2007a. Practical techniques for finite element modelling to simulate structural crashworthiness in ship collisions and grounding (part I: theory). Ships Offshore Struct. 2:69–80.

Paik JK. 2007b. Practical techniques for finite element modelling to simulate structural crashworthiness in ship collisions and grounding (part II: verification). Ships Offshore Struct. 2:81–85.

Papanikolaou A, Bulian G, Mains C. 2015. GOALDS – goal based damaged stability: collision and grounding damages. Proceedings of the 12th International Ship Stability Workshop.

Pedersen P, Zhang S. 2000. Absorbed energy in ship collisions and grounding. J Ship Res. 44:140–154.

SOLAS. 2020. Subdivision, watertight and weathertight integrity, SOLAS Chapter II-1, Part B-2. International Convention for the Safety of Life at Sea, International Maritime Organization, London, UK.

Törnqvist R. 2003. Design of crashworthy ship structures, PhD Thesis, Department of Mechanical Engineering, Technical University of Denmark.

Simonsen BC, Ocakli H. 1999. Experiments and theory on deck and girder crushing. Thin Walled Struct. 34(3):195–216. doi:10.1016/S0263-8231(99)00015-4

Van de Graaf B, Broekhuijsen J, Vredeveldt A, Van de Ven A. 2004. Construction aspects for the Schelde Y-shape crashworthy hull structure, Society of Naval Architects of Japan (Ed.) Proceedings of the 3rd International Conference on Collision and Grounding of Ships, ICCGS 2004, October 25-27, 2004, Izu, Japan. 229–233.

Wierzbicki T, Abramowicz W. 1983. On the crushing mechanics of thin-walled structures. J Appl Mech. 50(4a):727–734.

Woisin G. 1979. Structural design against collision effects. Shiff und Hafen.

Zhang S. 1999. The mechanics of ship collision. PhD Thesis, Department of Naval Architecture and Offshore Engineering, Technical University of Denmark.

Appendix

This appendix presents the main results obtained during a benchmark study carried out with the objective of comparing different methods (super-elements and finite elements), software (SHARP, MarcolXMF, LS-Dyna) and assumptions under various collision and grounding situations. For the purpose of the present paper, the results pertaining to SHARP against reference LS-Dyna results are provided. Full results are to be found in Le Sourne et al. (2021) and Kim et al. (2021b).

For the benchmark study, the considered vessels are illustrated in Figure A1, and Table A1 presents their main particulars.

In the collision benchmark study, four scenarios have been considered, see Figure A2 and Table A2.

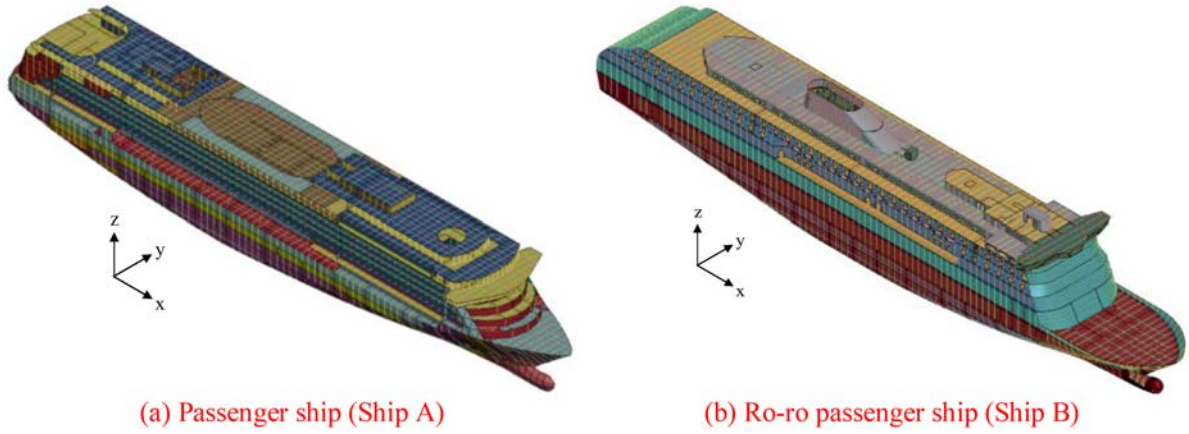

Figure A1. Target ships used in the benchmark study (This figure is available in colour online).

Table A1. Main dimensions of target ships.

Particular	Ship A	Ship B
Overall length [m]	238.0	221.5
Moulded breadth [m]	32.2	30.0
Depth [m]	16.0	15.2
Design draft [m]	7.2	6.9
Displacement [tonne]	Approx. 34,000	Approx. 30,000
Block coefficient [-]	0.661	0.578

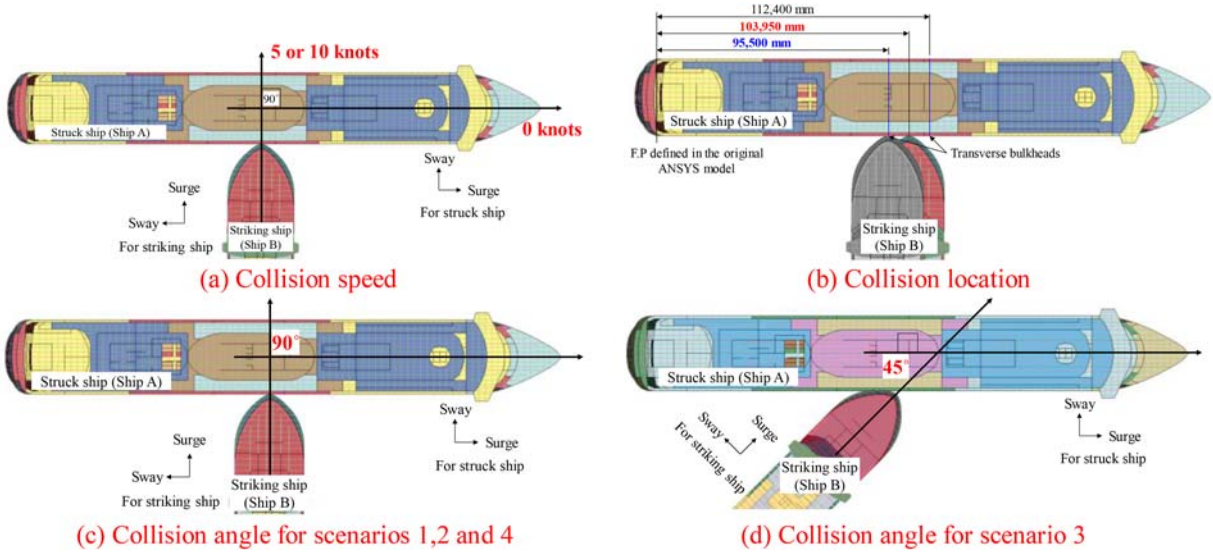

Figure A2. Definition of collision parameters (This figure is available in colour online).

In both super-elements (SHARP) and finite elements (LS-Dyna) methods, the hydrodynamic boundary conditions have been applied via MCOL, which accounts for (i) mass matrix, (ii) hydrodynamic restoring forces, (iii) added mass, (iv) buoyancy parameters and (v) wave damping forces as per Le Sourne et al. (2001). Accordingly, seakeeping parameters were calculated in 20 frequency steps (0.1–2.0 rad/s) in infinite water depth, assuming zero forward speed for the struck ship and a forward speed of 5 or 10 knots for the striking ship. The parameters considered to derive the effects of surrounding water are given in Table 11.

The main parameters and assumptions of the super-element and finite-element structural models are given in Table 12.

The summary results are shown in Figure A3, and penetration versus dissipated energy curves are shown in Figure A4 for each scenario. Overall, it is deemed that a very good agreement is obtained between the super-element simulation (SHARP) and the finite-element (LS-Dyna) simulation.

Table A2. Collision benchmark scenarios.

	Target ships				Collision location		
						Draft [m]	
Scenario No.	Striking	Struck	Collision angle [°]	Collision speed [knots]	Longitudinal from A.P. [m]	Ship A	Ship B
1	Ship B	Ship A	90	5	103.95	6.9	7.2
2			90	10	103.95		
3			45	5	103.95		
4			90	5	95.5		

Table A3. Main parameters to calculate the effects of surrounding water.

Parameter	Ship A	Ship B
Draft [m]	7.2	6.9
Displacement [tonne]	33,923	30,114
KG [m]	15.14	13.96
Gyration radius, x-direction [m]	11	11
Gyration radius, y-direction [m]	60	55
Gyration radius, z-direction [m]	61	55

Table A4. Main parameters and assumptions of structural models.

Parameter	SHARP	LS-Dyna
Resolution method	Super-elements	Finite-elements, explicit
FSI	MCOL	MCOL
Mesh size [mm]	–	120
Struck ship	Deformable	Deformable
Striking ship	Rigid	Deformable
Material curve	Rigid-perfectly plastic	Elastic-perfectly plastic
Material density [kg/m^3]	7850	7850
Young's modulus [MPa]	–	205,800
Yield strength [MPa]	–	235
Flow stress [MPa]	235	–
Dynamic effect	–	Cowper–Symonds
Fracture strain [–]	0.1	0.1
Friction coefficient	0.3	0.3

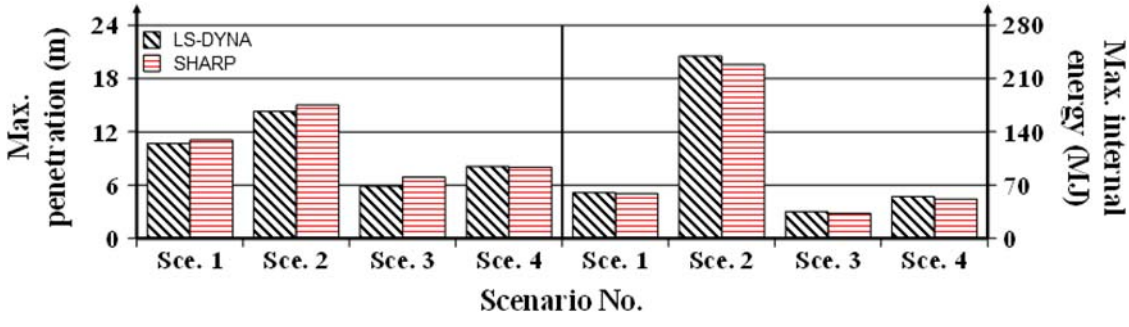

Figure A3. Comparison of maximum penetration and dissipated energy (This figure is available in colour online).

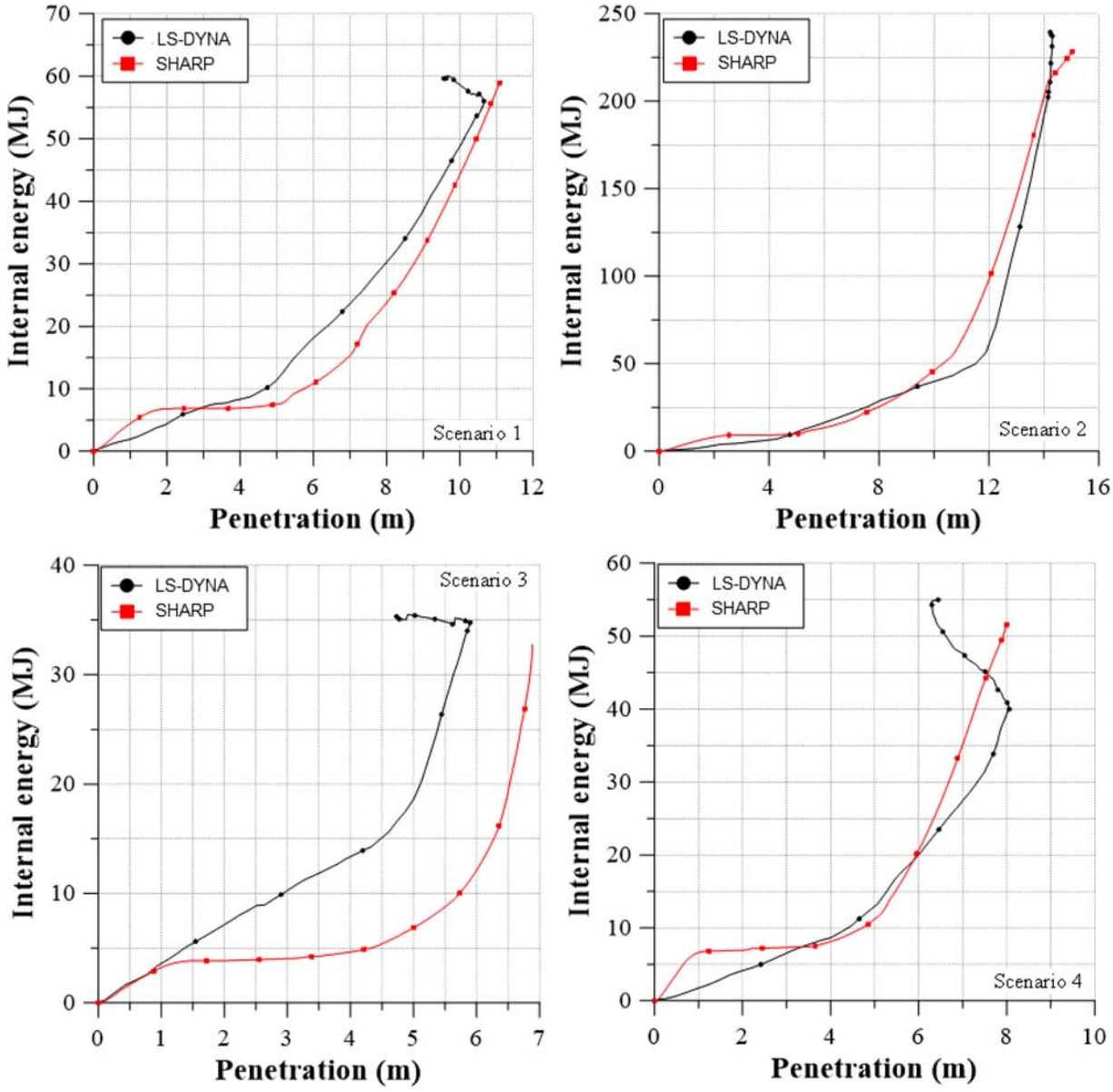

Figure A4. Comparison of penetration versus dissipated energy curves (This figure is available in colour online).